AJNR

Early MRI Characteristics after MRI-Guided Laser-Assisted Cingulotomy for Intractable Pain Control

S.H. Sundararajan, P. Belani, S. Danish and I. Keller

AJNR Am J Neuroradiol 2015, 36 (7) 1283-1287
doi: https://doi.org/10.3174/ajnr.A4289
http://www.ajnr.org/content/36/7/1283

Early MRI Characteristics after MRI-Guided Laser-Assisted Cingulotomy for Intractable Pain Control

S.H. Sundararajan, P. Belani, S. Danish, and I. Keller

ABSTRACT

BACKGROUND AND PURPOSE: Cingulotomy is a well-accepted stereotactic procedure in the treatment of debilitating pain syndromes. At our institution, we used a 980-nm diode laser to perform MR imaging–guided laser-assisted cingulotomy. We report the early MR imaging changes associated with this technique.

MATERIALS AND METHODS: In this retrospective analysis, MR imaging–guided laser-assisted cingulotomy was performed in 4 patients with intractable pain secondary to metastatic disease. Patients were imaged at various time points postprocedure, with visual analysis of MR imaging changes in the cingulate gyri during that timeframe.

RESULTS: Twenty-four hours postablation, 4 distinct zones of concentric rings reminiscent of an "owl eye" shape were noted in the cingulate gyri. Extrapolating from the imaging characteristics of the rings, we defined each zone as follows: The central zone (zone 1) represents a laser probe void with fluid, zones 2 and 3 have signal characteristics that represent hemorrhage and leaked protein, and zone 4 has a peripheral ring of acute infarction, enhancement, and surrounding edema. One patient with 1-year follow-up showed persistent concentric rings with resolution of enhancement and edema.

CONCLUSIONS: Post-MR imaging–guided laser-assisted cingulotomy rings appear to represent a continuum of injury created by the laser probe and thermal injury. The imaging changes are similar to those described for laser ablation of tumor-infiltrated brain with a 1064-nm laser. This is the first study to characterize early MR imaging changes after MR imaging–guided laser-assisted cingulotomy by using a 980-nm laser. It is important for neuroradiologists and neurosurgeons to understand expected imaging findings as laser ablation cingulotomy re-emerges to treat intractable pain.

ABBREVIATION: MRgLAC = MR imaging–guided laser-assisted cingulotomy

The cingulate gyrus is an important part of the limbic system and is involved in the emotional response to pain.[1] Anterior cingulotomy has been a well-accepted stereotactic procedure in the treatment of both refractory obsessive-compulsive disorder and debilitating pain syndromes.[2,3] The objective of cingulotomy is the severing of the supracallosal fibers of the cingulum bundle, which pass through the anterior cingulate gyrus.[4]

For several decades, the cingulate gyrus has been a surgical target to treat a variety of disorders.[5] In 1948, open cingulectomies were first described for the treatment of schizophrenia.[6] In 1962, pneumoencephalographic guidance for performing closed-cingulotomy was introduced by Foltz and White[7] for pain. In 1973, Balasubramaniam et al[8] described the technique of stereotactic cingulotomy in the management of patients with alcohol addiction. This frame-based stereotactic approach combined pneumoencephalographic and angiographic guidance for well-defined resection of the cingulate gyri.

During the 1990s, early guidance techniques with the patient under general anesthesia were replaced by MR imaging guidance with the patient under local anesthesia. Since then, the procedure has been performed by using a radiofrequency probe with or without MR imaging stereotaxis.[9] Hassenbusch et al[10] created a spheric radiofrequency lesion in 4 patients by applying 75°C for 60 seconds by using this technique, for which he reported significant improvement of intractable pain. At our institution, we have recently introduced the use of a 980-nm diode laser to perform MR imaging–guided laser-assisted cingulotomy (MRgLAC).

Received November 2, 2014; accepted after revision January 15, 2015.

From the Department of Radiology (S.H.S., P.B.), Rutgers-Robert Wood Johnson Medical School, New Brunswick, New Jersey; Departments of Neurosurgery (S.D.) and Radiology (I.K.), Rutgers-Robert Wood Johnson Medical School and University Hospital, New Brunswick, New Jersey; and University Radiology Group (I.K.), East Brunswick, New Jersey.

Please address correspondence to Sri Hari Sundararajan, MD, Robert Wood Johnson Medical School, Department of Radiology, MEB 404, One Robert Wood Johnson Pl, New Brunswick, NJ 08903-0019; e-mail: ssundararajan@univrad.com; @radiolosri

http://dx.doi.org/10.3174/ajnr.A4289

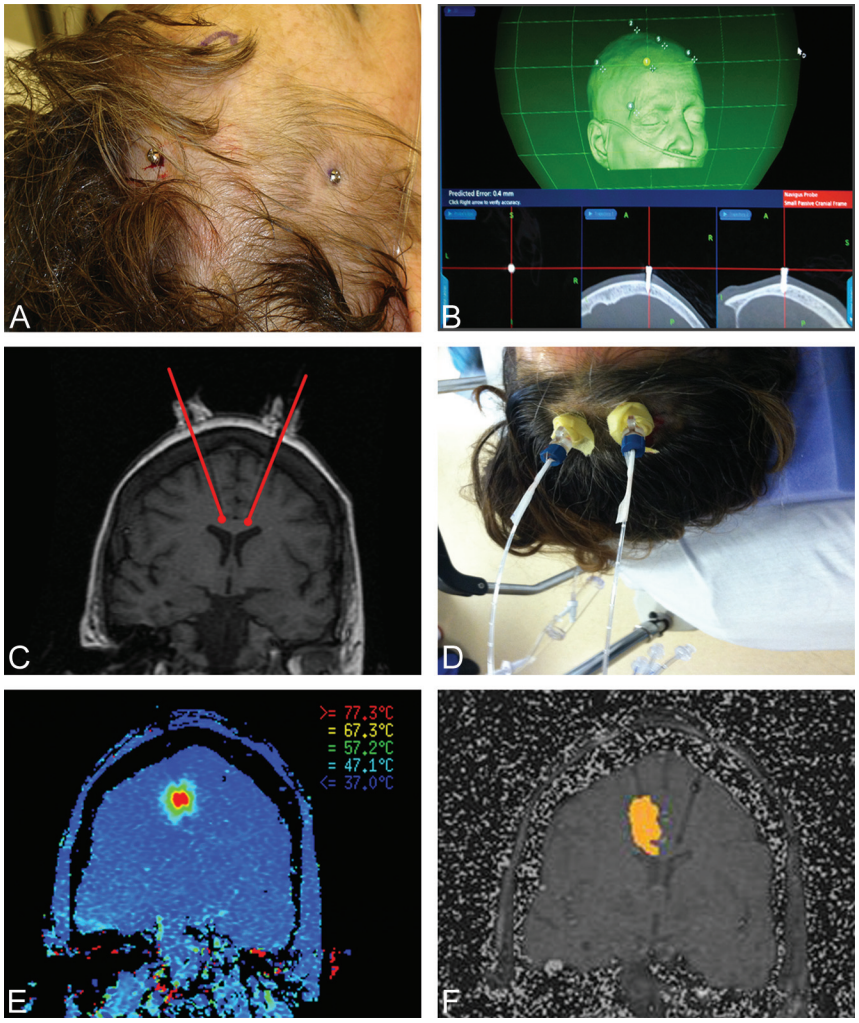

FIG 1. Fiducial markers are placed (*A*) with follow-up registration imaging performed for confirmed localization (*B*). Alignment of the navigation probe within a precision aiming device is ensured before it is locked into position (*C* and *D*). Thermal localization is performed to estimate approximate temperatures to be reached during MRgLAC to ensure that the temperature does not exceed 90°C. This is demonstrated by color gradients representing measured temperature gradients (*E*). Sequential real-time images obtained during MRgLAC of the right cingulum are then acquired. Note placement and location of the probes in both gyri and a steadily increasing region of thermal ablation in the right cingulate (*F*).

Patient demographics

Patient No.	Age (yr)	Sex	Metastatic Neoplasm	Post-MRgLAC Follow-Up
1	47	Female	Liposarcoma	24 hours
2	38	Female	Breast	24 hours
3	51	Female	Colon	24 hours
4	82	Female	Colon	1 year

MR imaging findings in patients after laser ablative cingulotomy have been previously described.[9-12] However, these studies reported only T1- and T2-weighted imaging features and lacked discussion of potential etiologies and evolution of reported signal changes. The multisequential MR imaging characteristics of laser-guided cingulotomy for patients with intractable pain have not been previously characterized, to our knowledge. The purpose of this study was to report the early MR imaging changes associated with cingulotomy by using a 980-nm diode laser. Our descriptions are based on the original work by Spangler et al,[11] who, in 1996, described the postoperative MR imaging characteristics of cingulotomies for the treatment of psychiatric disorders.

MATERIALS AND METHODS

Between 2012 and 2013, 4 patients were selected for laser ablation cingulotomy. These patients had systemic metastatic cancer, with a life expectancy of fewer than 6 months and intractable pain that was not relieved by conventional pain management. After review by a multidisciplinary tumor board, MRgLAC was offered as a palliative procedure for intractable pain management. All patients were enrolled in an institutional review board–approved protocol.

One-millimeter CT images (LightSpeed Pro 16; GE Healthcare, Milwaukee, Wisconsin) and postgadolinium axial T1 echo-spoiled gradient-echo and axial FLAIR MR images (Optima MR450w 1.5T with a GEM Suite; GE Healthcare) were obtained for preprocedural planning on a StealthStation S7 (Medtronic Navigation, Minneapolis, Minnesota). The FLAIR is a 2D sequence fused with the echo-spoiled gradient echo. This sequence is not necessary, but we have found it useful in certain cases in which the cingulate sulcus is not clearly visualized on the coronal reconstructions of the echo-spoiled gradient-echo sequence.

The targeting method was derived from that used by Richter et al.[13] Two ablations within each cingulate gyrus were planned. A target point was placed approximately 20 mm posterior to the tip of the frontal horn (y-coordinate), parallel with the roof of the lateral ventricle within the cingulate gyrus. The planning trajectory was made perpendicular to the long axis of the corpus callosum on the sagittal image.[14]

The patient was first placed under general anesthesia. After confirmation of the position and trajectory, an incision is made with a No. 15 scalpel. A twist drill craniotomy was created and used to pass the plastic bone anchor into the skull along the proper trajectory. Once in place, the laser-cooling catheter was passed to the appropriate depth and secured. The process was repeated on the contralateral side.[14]

The patient was transported with lasers in place to diagnostic MR imaging, where the laser catheters were connected to the Thermal Therapy System (Visualase, Houston, Texas). A T1 echo-spoiled gradient-echo coronal image was acquired as a reference image. We used an oblique coronal reference so that both ablations could be performed with the same reference image.

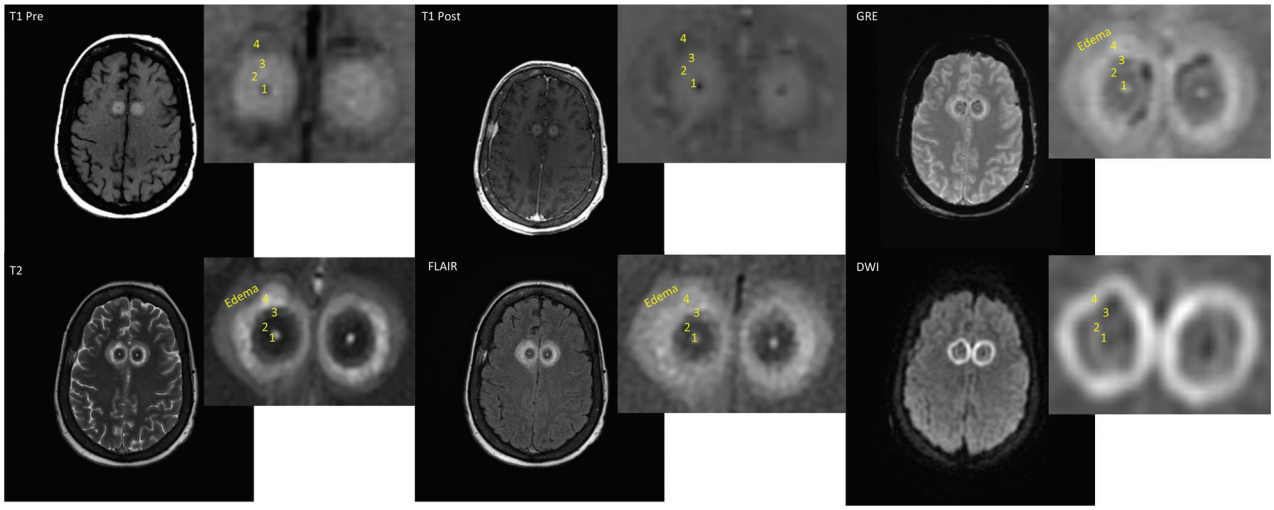

FIG 2. The above owl eye–appearing lesions are recorded 24 hours post-laser ablation of the cingulate gyri in patient 1. Four discrete zones are noted, labeled 1–4 from central to peripheral. All patients who underwent MRgLAC demonstrated this zonal distribution of signal abnormality.

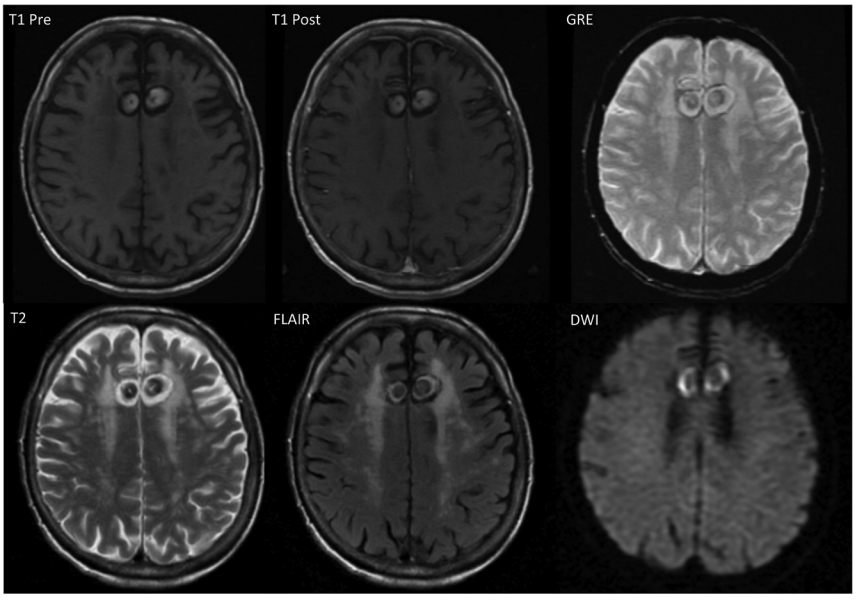

FIG 3. Imaging performed in patient 4 one year following MRgLAC demonstrates the persistent appearance of bilateral concentric zones of thermal ablation with a preserved owl eyes configuration. Note the lack of enhancement on postcontrast imaging, resolution of postprocedural edema, and T2-shinethrough on diffusion-weighted imaging.

High-temperature limits (90°C) were set near the tip of the applicators to avoid production of steam. Low temperature limits (50°C) were set at the borders of the target areas to avoid unintended thermal damage to nearby critical structures, such as the corpus callosum. Real-time thermal damage was estimated by an MR imaging pixel shift of the target tissue in response to thermal damage (Fig 1).[14,15]

Two ablations were performed in each cingulum. The initial ablation was made within the anterior cingulate gyrus. The inferior ablation boundary was the corpus callosum. Medially, the ablation was bounded by the pia mater of the gyrus. Laterally, the ablation was bounded by the limits of the thermal energy distribution. The second ablation was performed to incorporate the medial prefrontal cortex and medial white matter. The superior limit of the second ablation was kept below the subcortical U-fibers of the superior and middle frontal gyri. The total ablation volume within each cingulum was approximately 1.5 mL. Baseline immediate postablation imaging was performed at the conclusion of the procedure.

All patients were imaged immediately after and 24 hours after the procedure, with patient demographics as listed in the Table. Patient 4 unexpectedly survived, allowing 1-year follow-up imaging to be obtained in this patient also. Imaging sequences included T1, T1 postcontrast, T2, FLAIR postcontrast, gradient recalled-echo, DWI, and ADC mapping. Signal changes were graded as isointense, hypointense, or hyperintense relative to gray matter in the specific imaging sequence.

RESULTS

Postprocedural assessment of the 4 different patients after MRgLAC at 24 hours demonstrated a broad circular region of thermal-induced injury with 4 concentric rings in the bilateral cingulate gyri. These regions of varying signal intensity extended from the center to the periphery and were arbitrarily labeled zones 1–4 (Fig 2). These concentric rings persisted 1 year following thermal ablation in 1 patient (Fig 3).

Signal changes in the described zones were graded as hypointense, isointense, or hyperintense relative to the gray matter intensity of the sequence. Zone 1 demonstrated central T1 hypointensity with thin peripheral enhancement on postcontrast imaging. There was corresponding hyperintensity on T2 with correspondingly less intensity on FLAIR imaging. Gradient recalled-

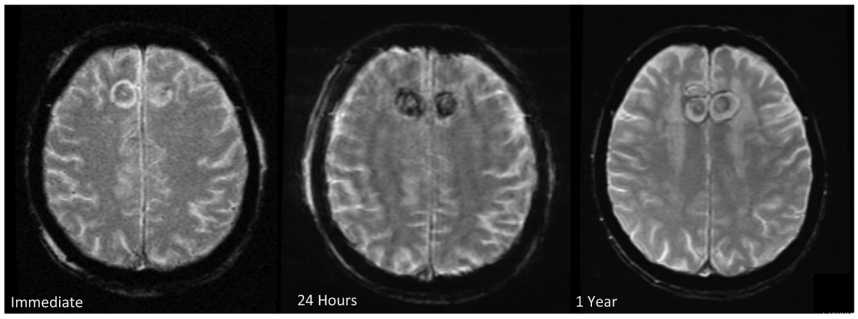

FIG 4. The following gradient recalled-echo images from patient 4 demonstrate evolution of postprocedural gradient-echo imaging changes related to MRgLAC. There is an interval increase in the magnetic susceptibility signal in zone 3 between the immediate and post-24 hour images. Note is made of residual peripheral magnetic susceptibility 1 year following the procedure.

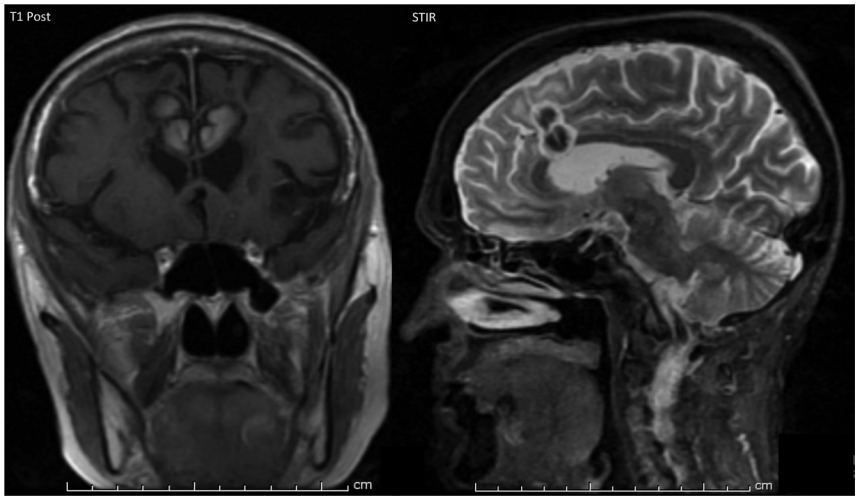

FIG 5. Coronal T1 postcontrast and sagittal STIR imaging performed on patient 4 one year following MRgLAC demonstrates 2 pairs of concentric rings in each cingulate. These correspond to the 2 adjacent areas of thermal ablation produced in each cingulum.

echo imaging showed no magnetic susceptibility in this location, and diffusion-weighted imaging showed no evidence of restricted diffusion in this location (Fig 2).

Zones 2 and 3 shared similar imaging characteristics. They were iso- to hyperintense on T1-weighted imaging and did not demonstrate enhancement on postcontrast imaging. A clearer distinction between zones 2 and 3 was noted on T2-weighted and FLAIR imaging, with a hypointense zone 2 and mixed hypo-/isointense zone 3 noted. Varying degrees of magnetic susceptibility were noted along the periphery of zone 3. No restricted diffusion was noted in either zone 2 or 3 (Figs 2 and 4).

Zone 4 was broader than the previously mentioned zones. The parenchyma within this zone demonstrated mixed iso-/hypointensity on T1-weighted imaging and was without enhancement on contrast-enhanced T1WI. Its characteristic signal properties included its true restricted diffusion with corresponding T2 and FLAIR hyperintensity. Variable magnetic susceptibility was seen, which could persist even up to 1 year. An ill-defined circumferential region of T2 and FLAIR hyperintensity corresponding to thermal-induced edema surrounded this zone. The 1-year follow-up MR imaging of patient 4 showed resolution of postprocedural edema, lack of enhancement on postcontrast imaging, and T2-shinethrough on diffusion-weighted imaging (Figs 2, 4, and 5).

DISCUSSION

Thermal ablation involves the deposition and absorption of light energy to generate controlled regions of volumetric heat distribution within a target tissue. Fiber optics are MR imaging–compatible and are used to target light energy deposition during thermal image-guided applications. The degree of volumetric heating induced within a given target tissue is determined by the wavelength of emitted light and the absorption peak of light of the target tissue at a given wavelength. The MR imaging concentric ring characteristics of thermal ablative therapy of the brain with radiofrequency ablation and 1048-nm lasers have been described previously. Those reports were based on imaging paradigms limited to T1 and T2 sequences obtained without gadolinium.[9-12]

Several notable factors distinguish our case series from previously reported thermal-ablative changes. Our retrospective study was performed on 4 patients who underwent MR imaging–guided laser ablation cingulotomy by using a state-of-the-art 980-nm laser. Radiofrequency ablation intracranial 1048-nm lasers are produced by a neodymium-doped yttrium aluminum garnet source. While they are effective in producing controlled zones of thermal ablation, some factors limiting their widespread utility include the high current consumption of the source, a power requirement of up to 220 V, and the need for active water cooling. In contrast, diode-based lasers producing lasers at a wavelength of 980 nm are capable of producing fast, precise, and tighter zones of ablation. Diode-based sources use semiconductors that lower both the laser's power requirement to 110 V and cooling requirement to air cooling. Furthermore, the absorption coefficient for water with a 980-nm laser being 3 times higher than that with a 1048-nm laser (0.482 versus 0.144 cm^{-1}) allows a greater rate of heating per unit of time.[16]

Our imaging sequences were also more extensive than the ones previously applied and included both pre- and postgadolinium sequences. This change allowed improved characterization of the lesions. T1, T2, postcontrast TI, FLAIR, gradient recalled-echo, and DWI pulse sequences were used in this study. The zones of thermal injury were evaluated within 24 hours of surgery in all our patients. Long-term follow-up imaging in these patients was not performed because our patient life expectancy for this pilot study was fewer than 6 months. However, patient 4 survived beyond the

estimated life expectancy and was able to undergo follow-up imaging.

Four concentric zones of injury were identified on axial plane imaging. The 2 regions of thermal ablation produced in each cingulum are best appreciated on sagittal and coronal planes (Fig 3).

Zone 1 (the central zone) demonstrated hypointense signal on noncontrast T1WI and FLAIR sequences with corresponding rim enhancement on the postgadolinium FLAIR sequence. These findings represent a CSF-filled cleft produced by the void of the probe that is removed after ablation. Zones 2 and 3 demonstrated heterogeneous T1 signal without significant enhancement. Acute blood products may contribute to T1 shortening as denoted by the evolution of magnetic susceptibility in these zones. However, we believe the increased T1 signal in these zones is more related to leakage of intracellular proteins, given the relative discordance with corresponding magnetic susceptibility on gradient-echo imaging in some patients (Figs 2 and 4).

Zone 4 demonstrates restricted diffusion with associated hypointensity on ADC and patchy enhancement. Gross specimens from tissues treated with a 980-nm laser show hyperemic rings along the outermost margin of an ablated site that histologically represents thermal necrosis.[16] As such, the noted signal changes in zone 4 are more suggestive of true infarction of the outermost layer, with patchy enhancement in this location likely related to a combination of postprocedural enhancement and enhancement from subacute infarction.

Unexpected imaging of patient 4 performed 1 year after MRgLAC confirmed this maintained zonal distribution. This follow-up imaging also showed resolution of postprocedural edema and maturation of zone 4 infarction, as noted by the lack of enhancement on postcontrast imaging and the lack of true restricted diffusion (Fig 3).

CONCLUSIONS

MRgLAC is a newly introduced technique to perform bilateral anterior cingulotomy for intractable pain control. The perioperative imaging changes seem similar to those described for laser ablation of tumor-infiltrated tissue with a 1064-nm laser. This is the first study to characterize early MR imaging changes after MRgLAC by using a 980-nm laser. We plan to expand this description by adding time points to the follow-up imaging and characterization of additional patients with future planned studies.

Disclosures: Shabbar Danish—*UNRELATED: Payment for Lectures (including service on Speakers Bureaus)*: Medtronic, *Comments*: received honoraria as a faculty member for training courses.

REFERENCES

1. Vogt BA. **Pain and emotion interactions in the subregions of the cingulate gyrus.** *Nat Rev Neurosci* 2005;6:533–44
2. Harsh V, Viswanathan A. **Surgical/radiological interventions for cancer pain.** *Curr Pain Headache Rep* 2013;17:331
3. Christmas D, Morrison C, Eljamel M, et al. **Neurosurgery for mental disorders.** *Adv Psychiatr Treat* 2004;10:189–99
4. Yen CP, Kuan CY, Sheehan J, et al. **Impact of bilateral anterior cingulotomy on neurocognitive function in patients with intractable pain.** *J Clin Neurosci* 2009;16:214–19
5. Brotis AG, Kapsalaki EZ, Paterakis K, et al. **Historic evolutions of open cingulectomy and stereotactic cingulotomy in the management of medically intractable psychiatric disorders, pain and drug addiction.** *Stereotact Funct Neurosurg* 2009;87:271–91
6. Ward AA Jr. **The anterior cingulate gyrus and personality.** *Res Publ Assoc Res Nerv Ment Dis* 1948;27:438–45
7. Foltz EL, White LE Jr. **Pain 'relief' by frontal cingulotomy.** *J Neurosurg* 1962;19:89–100
8. Balasubramaniam V, Kanaka TS, Ramanujam PB. **Stereotaxic cingulomotomy for drug addiction.** *Neurol India* 1973;21:63–66
9. De Salles AA, Brekhus SD, De Souza EC, et al. **Early postoperative appearance of radiofrequency lesions on magnetic resonance imaging.** *Neurosurgery* 1995;36:932–36; discussion 936–37
10. Hassenbusch SJ, Pillay PK, Barnett GH. **Radiofrequency cingulotomy for intractable cancer pain using stereotaxis guided by magnetic resonance imaging.** *Neurosurgery* 1990;27:220–23
11. Spangler WJ, Cosgrove GR, Ballantine HT Jr, et al. **Magnetic resonance image-guided stereotactic cingulotomy for intractable psychiatric disease.** *Neurosurgery* 1996;38:1071–76; discussion 1076–78
12. Schwabe B, Kahn T, Harth T, et al. **Laser-induced thermal lesions in the human brain: short- and long-term appearance on MRI.** *J Comput Assist Tomogr* 1997;21:818–25
13. Richter EO, Davis KD, Hutchison WD, et al. **Cingulotomy for psychiatric disease: microelectrode guidance, a callosal reference system for documenting lesion location, and clinical results.** *Neurosurgery* 2004;54:622–28; discussion 628–30
14. Jethwa PR, Barrese JC, Gowda A, et al. **Magnetic resonance thermometry-guided laser-induced thermal therapy for intracranial neoplasms: initial experience.** *Neurosurgery* 2012;71(1 suppl operative):133–44; 144–45
15. Rieke V, Pauly KB. **MR thermometry.** *J Magn Reson Imaging* 2008; 27:376–90
16. Ahrar K, Gowda A, Javadi S, et al. **Preclinical assessment of a 980-nm diode laser ablation system in a large animal tumor model.** *J Vasc Interv Radiol* 2010;21:555–61